Available online at www.sciencedirect.com
ScienceDirect
Journal of the European Ceramic Society 27 (2007) 3803–3806
www.elsevier.com/locate/jeurceramsoc

Electron trapping of laser-induced carriers in Er-doped SnO_2 thin films

E.A. Morais [a,b], L.V.A. Scalvi [a,*]

[a] D. Fisica-FC, UNESP, Un. Estadual Paulista, C.P. 473, 17033-360 Bauru, SP, Brazil
[b] Progr. Pós-Graduação em Ciência e Tecnologia de Materiais, UNESP, SP, Brazil

Available online 26 March 2007

Abstract

In order to investigate optically excited electronic transport in Er-doped SnO_2, thin films are excited with the fourth harmonic of an Nd:YAG laser (266 nm) at low temperature, yielding conductivity decay when the illumination is removed. Inspection of these electrical characteristics aims knowledge for electroluminescent devices operation. Based on a proposed model where trapping defects present thermally activated cross section, the capture barrier is evaluated as 140, 108, 100 and 148 meV for doped SnO_2 thin films with 0.0, 0.05, 0.10 and 4.0 at% of Er, respectively. The undoped film has vacancy levels as dominating, whereas for doped films, there are two distinct trapping centers: Er^{3+} substitutional at Sn^{4+} lattice sites and Er^{3+} located at grain boundary.

Keywords: Tin dioxide films; Sol–gel; Erbium doping

1. Introduction

Incorporation of erbium ion (Er^{3+}) in semiconductors may contribute for technological innovation and offers the possibility of very significant applications in optical communication, since it has one emission at 1.54 μm, coincident with the minimum absorption of silica-based optical fibers.[1] This luminescence leads to a potential use in waveguides and electroluminescent emitters. The emission at room temperature is related with phonon-assisted transitions, which decrease the photoluminescence (PL) intensity about room temperature. This PL quenching decreases with bandgap energy, making rare-earth doping of wide bandgap semiconductors a very attractive process.[2] It includes the n-type wide bandgap semiconductor SnO_2.

The knowledge of optically excited electrical characteristics in Er-doped SnO_2 is fundamental for design and operation of electroluminescent devices. The optical ionization of Er-related defects and the analysis of charge trapping back help this investigation, since it combines optical and electrical properties of Er-doped SnO_2 thin films. In tin dioxide, oxygen vacancies act as donors centers. Two donor levels associated with this center have been reported, a shallow level at 30 meV below the conduction band and a deep level about 150 meV.[3] Er^{3+} is incorporated into SnO_2 lattice substitutional in Sn^{4+} sites and exhibits an acceptor like behavior in tin dioxide,[4] leading to a high degree of electrical charge compensation, and high resistivity films. Ion incoporation at grain boundary, caused by low solubility limit of rare earths in SnO_2 (less than 0.1 mol%), may also contribute for high resistivity.[5] Recombination of electron-hole pairs with desorbed oxygen species leads to persistent photoconductivity (PPC) effect[6] in undoped SnO_2 sol–gel thin films at low temperature.[4] Our deeper investigation in the range 200–300 K, reported here, shows a small, but measurable decay of the photo-induced conductive metastable state in undoped SnO_2 thin films.

In this paper, the decay of photo-excited conductivity is applied in order to understand the electron trapping phenomena. The experiment may be summarized as follows: laser light (266 nm) has above bandgap energy and may create electron-hole pairs and ionize intra-bandgap defects: substitutional Er^{3+}, grain boundary located Er^{3+} and oxygen vacancy. After removing the illumination, the time-temperature dependence of charge carrier trapping by defects is measured and the thermally activated capture cross section of the dominating level is evaluated. Results include undoped and Er-doped SnO_2 thin films, deposited by sol–gel-dip-coating (SGDC) process.

2. Experimental

The desired amount of $ErCl_3{\cdot}6H_2O$ was added to an aqueous solution of $SnCl_4{\cdot}5H_2O$ (0.5 mol l^{-1}), under stirring with a magnetic bar, followed by addition of NH_4OH until pH

* Corresponding author. Tel.: +55 14 3103 6084; fax: +55 14 3103 6094.
E-mail address: scalvi@fc.unesp.br (L.V.A. Scalvi).

0955-2219/$ – see front matter © 2007 Elsevier Ltd. All rights reserved.
doi:10.1016/j.jeurceramsoc.2007.02.037

reaches 11. Ions Cl^- and NH_4^+ were eliminated by dialysis. Films were deposited on silicate glass substrates by dip-coating with 10 cm/min dip rate. Multi-dipped films were continuously deposited at room temperature with firing at 400 °C for 10 min after each dip. Resulting film (10 layers) was annealed at 550 °C for 1 h.

Sn electrodes were deposited on the samples by resistive evaporation technique, through a shadow mask in an Edwards evaporator system, model Auto 306, under a pressure of about 10^{-6} Torr. In this procedure the crucible is heated by a high electrical current. Electrodes are annealed to 200 °C by 20 min. Low temperature electrical measurements were done in a He-closed cycle Janis Cryostat that controls sample temperature in the range 10–300 K within 0.05 K of precision. For the decay of photo-induced conductivity measurements, samples were irradiated with the fourth harmonic (266 nm) of an Nd:YAG pulsed laser, with 4.8 mJ of energy and 10 Hz of pulse frequency, by 10 min, keeping constant temperature.

3. Results–discussion

Normalized conductivity as function of time is shown in Fig. 1 for an undoped SnO_2 film, after the film is excited by the Nd:YAG laser (266 nm line). The decay becomes slower as the temperature decreases, leading to the PPC phenomena observed at low temperature (mainly at 70 K).[4] The inset of Fig. 1 shows the normalized conductivity plotted as function of time for distinct pressures. The faster decay for higher pressures assures that this mechanism is helped by electron capture at oxygen species adsorbed at grain boundaries and surface. As the atmosphere becomes cleaner of oxygen, due to the vacuum pump, the decay becomes slower because there is less oxygen to get adsorbed and contribute to capture. Then the electron capture becomes completely dominated by vacancies for low pressures.

Fig. 2 shows the decay of photo-excited conductivity at several temperatures for SnO_2 doped with distinct Er doping. Fig. 2(a) shows these data for SnO_2 doped with 0.05 at% of Er. The decay of photo-excited conductivity for SnO_2 doped with

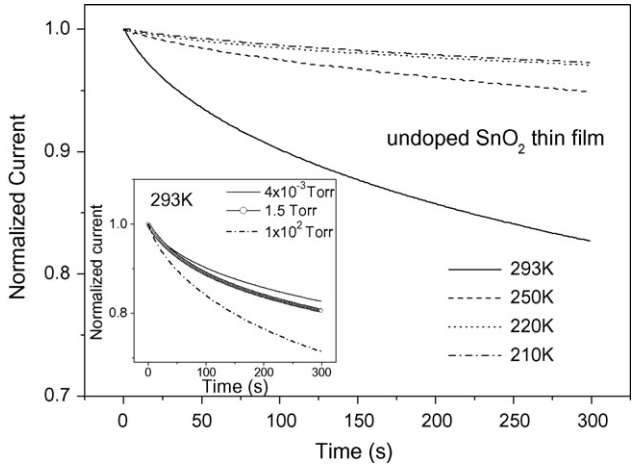

Fig. 1. Decay of photo-excited conductivity at several temperatures for undoped SnO_2 thin film. Inset—decay of photo-excited conductivity at several pressures for the same film.

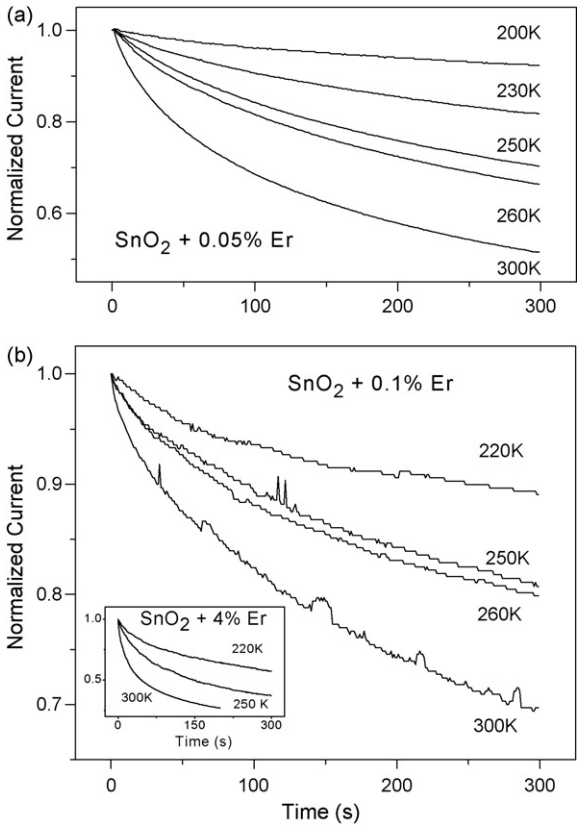

Fig. 2. (a) Decay of photo-excited conductivity at several temperatures for SnO_2:0.05% Er. (b) Decay of photo-excited conductivity at several temperatures for SnO_2:0.10% Er. Inset—data for SnO_2:4% Er.

0.10 at% of Er is shown in Fig. 2(b) and the inset of Fig. 2(b) shows this decay for SnO_2 doped with 4 at% of Er. As it can be observed, as the temperature increases the decay becomes faster, for the same Er doping concentration. Comparing this data set, it can be observed that the decay rate becomes slower for the lower Er concentration.

The observed decay of conductivity as function of time means that the resistance of the film increases with time. The decay of photo-induced electrons (n) from the conduction band to the trapping defect is given by[6]:

$$\frac{dn}{dt} = -C_n N_{Def}^{+} \tag{1}$$

where $C_n = V_{th}\gamma_n n$, V_{th} is the thermal velocity of free electrons, $\gamma_n = \gamma_\infty \exp(-E_{cap}/kT)$ is the capture cross section, E_{cap} is the potential barrier for electron trapping and γ_∞ is the constant capture cross section (infinite temperature). N_{Def}^{+} is the number of ionized defects. In this paper we analyze two kinds of defects: oxygen vacancies (V_O^+) and acceptor like erbium levels (Er^{3+}). Supposing that both centers are singly ionized, then: $N_{Def}^{o} \rightarrow e^- + N_{Def}^{+}$ and then $N_{Def}^{+} = n$, where it is considered that decay time is long enough to neglect electron-hole recombination. Besides, during the trapping process, V_O^+ and Er^{3+} levels present different capture times. Comparing Figs. 1 and 2, it is easily verified that the decay is faster for doped films (Er^{3+} levels dominating). Eq. (1) is a simple differential equation, with

trivial solution, given by:

$$n = \frac{n(0)}{(1 + n(0)V_{th}\gamma_n t)} \quad (2)$$

where $n(0)$ is the initial free electron concentration. Considering that mobility (μ) is dominated by the grain boundary scattering, we may neglect bulk scattering mechanisms (phonon and ionized impurity). X-ray diffraction data for these films (not shown) exhibits a diffuse shape profile, typical of small crystallite domain. The average crystallite size evaluate from line broadening XRD pattern is about 5 nm. Then, electrical transport dominated by grain boundary scattering is an adequate hypothesis since the grain size is very small. The mobility due to grain boundary scattering is proportional to $T^{-1/2}\exp(-\phi k^{-1}T^{-1})$,[7] where ϕ is the grain boundary potential barrier for scattering. Substituting these definitions into time-dependent resistance, one obtains:

$$R(t) = \frac{K_R}{qn\mu} = C_x + \frac{K_R T(3k/m^*)^{1/2}\gamma_\infty \exp(-(E_{cap} - \phi)/kT)t}{Aq} \quad (3)$$

where K_R is the proportionality constant between resistivity and resistance and A is the grain boundary scattering constant.[7] $C_x = T^{1/2}K_R\exp(\phi k^{-1}T^{-1})/[Aqn(0)]$ is temperature dependent but not time dependent. Eq. (3) means that $R(t)$ must be a linear function of time for fixed temperature. Evaluating the first derivative and calling it as slope, we get:

$$\frac{dR}{dt} = \text{slope} = K_f T \exp\left[-\frac{E_{cap} - \phi}{kT}\right] \quad (4)$$

where K_f is $\gamma_\infty(3\,k/m^*)^{1/2}K_R/(Aq)$. Therefore a plot of $\ln(\text{slope}/T)$ as function of $1/T$ yields the quantity $(E_{cap} - \phi)$ directly from the curve inclination. In our results ϕ is considered as a constant value (30 meV).[7] However, above the saturation limit, doping ions are mostly located at grain boundary, which must change the grain boundary potential barrier.

A plot of resistance as function of time is shown in Fig. 3 for SnO_2:0.05% Er as an example of resistance behavior for short times. For the other compositions (0.0, 0.1 and 4%) the curves are quite similar and they are not shown. The linear nature of the curve for short times is clearly observed in Fig. 3. Very low deviation from the linear behavior is observed.

A plot of $\ln(\text{slope}/T) \times T^{-1}$ curves, in accordance with Eq. (4), is shown in Fig. 4 for all the measured samples. The inset of Fig. 4 is the room temperature resistivity of the samples as function of Er doping. Evaluated values for $(E_{cap} - \phi)$ are shown in Table 1. Taking into account $\phi = 30$ meV,[7] the capture barrier is also evaluated. The capture barrier decreases with Er doping and increases for the highly saturated value of 4 at% Er. For the undoped sample, the evaluated value of $E_{cap} = 140$ meV, is in good accordance with the value obtained for the ionization level of vacancies.[3] The introduction of Er decreases the main observed capture barrier for the dominant deep level until the solubility limit has reached (between 0.05 and 0.10 at.% Er). As we have concluded previously,[5] the excess of Er is mainly

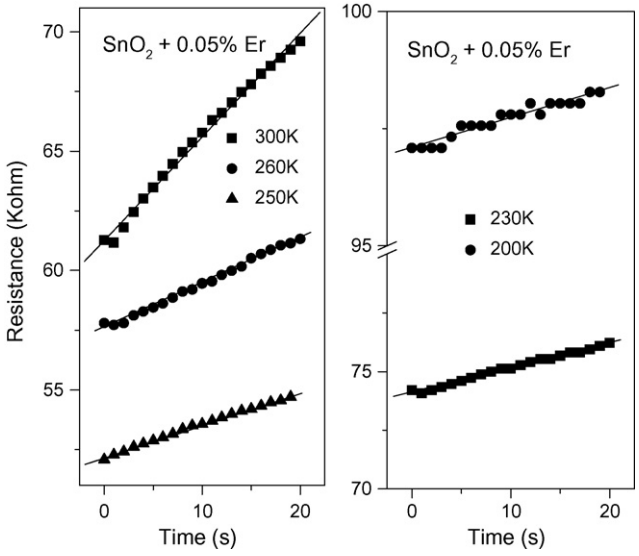

Fig. 3. Resistance as function of time and linear data fit at short times for SnO_2:0.05% Er.

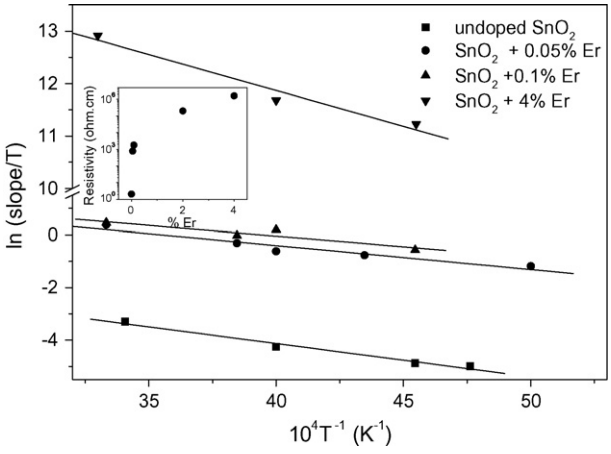

Fig. 4. Plot of $\ln(\text{slope}/T)$ as function of reciprocal temperature, according to theory developed in this paper for SnO_2 doped with several Er compositions. Inset—film resistivity as function of Er composition at 300 K.

located at grain boundary surface. Then, the time-temperature conductivity decay observed in Fig. 2 corresponds to capture by two different dominant trapping centers: substitutional Er^{3+} at Sn^{4+} lattice sites for SnO_2 doped with Er below the saturation limit and Er^{3+} at grain boundary for SnO_2:4% Er. Anyhow these possibilities are related, since the higher Er concentration at grain boundary must also increase the potential barrier at grain interface, and then, the value of 30 meV for ϕ. It is

Table 1
Potential barriers obtained from the decay and Arrhenius plot

Er composition (at%)	$E_{cap} - \phi$ (meV)	E_{cap} (meV)	E_a (meV)
0.00	110	140	144[a]
0.05	78	108	82
0.10	70	100	73
4.00	118	148	–

[a] From Ref. [8].

very interesting to notice the agreement between ($E_{cap} - \phi$) and the activation energy (E_a) obtained from the Arrhenius plot for Er-doped SnO_2 as shown in Table 1. The value for E_a of the undoped film is taken from a previous report[8] for comparison. For electron trapping by vacancies the E_{cap} becomes comparable with E_a. These results mean that the activation energy obtained from the conventional procedure through Arrhenius plot may be incorrect for materials with nanoscopic grains, because the potential barrier at grain boundary (ϕ) becomes comparable to the thermally activated capture barrier (E_{cap}). The high resistivity is related to the compensation between vacancies, which act as donors in the naturally n-type sample and the acceptor like nature of Er centers. The SnO_2:4 at.% Er is a highly compensated film. Films with lower Er doping (0.10 and 0.05 at%) may be considered as completely degenerated semiconductors in the photo-induced metastable state. The procedure used here takes into account that trapping defects present some sort of lattice relaxation.[6] For Er-doped SnO_2 films this relaxation is not clear up to this point because the trapping may induce a charge displacement when the acceptor Er becomes negatively charged. This issue is under investigation.

4. Conclusion

The understanding of photo-induced electrical properties of Er-doped SnO_2 is essential towards a complete description of electroluminescent centers present in this material. Er-doped SnO_2 thin films are very resistive due to charge compensation. From a theoretical data-fitting procedure, we conclude that Er^{3+} related centers present thermally activated capture cross section. The capture barrier (E_{cap}) shows different values whether the defect is substitutional to Sn^{4+} site or located at grain boundary. The decay of photo-excited conductivity is temperature and concentration dependent. Undoped samples also present a conductivity decay behavior, which is faster for higher temperature and higher pressure. Evaluation of E_{cap} for undoped thin film leads to a value very close to a deep ionization energy of vacancies.

The activation energy (E_a) obtained from Arrhenius plot agrees with the quantity ($E_{cap} - \phi$) for Er-doped films. Then the Arrhenius plot must be carefully used in samples with nanoscopic grains, because the potential barrier at grain boundary (ϕ) becomes comparable to the thermally activated capture barrier (E_{cap}).

Acknowledgements

The authors wish to thank Prof. Sidney J.L. Ribeiro for very fruitful discussions, and Dr. Viviany Geraldo for the undoped SnO_2 sample. They also acknowledge CAPES, CNPq and FAPESP for financial support.

References

1. Franzò, G., Priolo, F., Coffa, S., Polman, A. and Carrera, A., Room-temperature electroluminescence from Er-doped crystalline Si. *Appl. Phys. Lett.*, 1994, **64**, 2235–2237.
2. Casero, R. P., Liorente, A. G., Y-Moll, O. P., Seiller, W., Deforneau, R. M., Defornoeau, D. *et al.*, Er-doped ZnO thin films frown by pulsed laser deposition. *J. Appl. Phys.*, 2005, **97**, 054905-1-8.
3. Samson, S. and Fonstad, C. G., Defect structure and electronic donor levels in stannic oxide crystals. *J. Appl. Phys.*, 1973, **44**, 4618–4621.
4. Morais, E. A., Scalvi, L. V. A., Geraldo, V., Scalvi, R. M. F., Ribeiro, S. J. L., Santilli, C. V. *et al.*, Electro-optical properties of Er-doped SnO_2 thin films. *J. Eur. Ceram. Soc.*, 2004, **24**, 1857–1860.
5. Morais, E. A., Ribeiro, S. J. L., Scalvi, L. V. A., Santilli, C. V., Ruggiero, L. O., Pulcinelli, S. H. *et al.*, Optical characteristics of Er^{3+}–Yb^{3+} doped SnO_2 xerogels. *J. Alloys Compd.*, 2002, **344**, 217–220.
6. Dobson, T. W., Scalvi, L. V. A. and Wager, J. F., Transient decay of persistent photoconductivity in $Al_{0.3}Ga_{0.7}As$. *J. Appl. Phys.*, 1990, **68**, 601–605.
7. Zhang, D. H. and Ma, H. L., Scattering mechanisms of charge carriers in transparent conducting oxide films. *Appl. Phys. A*, 1996, **62**, 487–492.
8. Geraldo, V., Scalvi, L. V. A., Morais, E. A., Santilli, C. V. and Pulcinelli, S. H., Sb doping effects and oxygen adsorption in SnO_2 thin films deposited via sol–gel. *Mater. Res.*, 2003, **6**, 451–456.